PHYSICAL REVIEW D **78,** 074019 (2008)

Next-to-next-to-leading order QCD contributions to the flavor nonsinglet sector of $F_2(x, Q^2)$

Ali N. Khorramian* and S. Atashbar Tehrani+

Physics Department, Semnan University, Semnan, Iran
and School of Particles and Accelerators, IPM (Institute for Studies in Theoretical Physics and Mathematics), P.O. Box 19395-5531, Tehran, Iran

(Received 21 May 2008; revised manuscript received 2 September 2008; published 17 October 2008)

We present the results of our QCD analysis for nonsinglet unpolarized quark distributions and structure function $F_2(x, Q^2)$. New parameterizations are derived for the nonsinglet quark distributions for the kinematic wide range of x and Q^2. The analysis is based on the Jacobi polynomials expansion of the structure function. The higher twist contributions of proton and deuteron structure function are obtained in the large x region. Our calculations for nonsinglet unpolarized quark distribution functions based on the Jacobi polynomials method are in good agreement with the other theoretical models. The values of $\Lambda_{\rm QCD}$ and $\alpha_s(M_z^2)$ are determined.

DOI: 10.1103/PhysRevD.78.074019 PACS numbers: 13.60.Hb, 12.39.−x, 14.65.Bt

I. INTRODUCTION

The deep-inelastic lepton–nucleon scattering is the source of important information about the nucleon's structure. New and very precise data on nucleon structure functions have had a profound impact on our knowledge of parton distributions, in the small and large x region. During the last years the accuracy of the obtained experimental data has extensively grown up enough to study in detail the status of the comparison of the available data with the theoretical predictions of quantum chromodynamics (QCD) in the different regions of momentum transfer.

The importance of deep-inelastic scattering (DIS) for QCD goes well beyond the measurement of α_s [1]. In the past it played a crucial role in establishing the reality of quarks and gluons as partons and in promoting QCD as the theory of strong interactions. Nowadays it still generates challenges to QCD as, for example, in the domain of structure functions at small x [2,3] or of polarized structure functions [4] or of generalized parton densities [5] and so on.

All calculations of high energy processes with initial hadrons, whether within the standard model or exploring new physics, require parton distribution functions (PDF's) as an essential input. The reliability of these calculations, which underpins both future theoretical and experimental progress, depends on understanding the uncertainties of the PDF's. The assessment of PDF's, their uncertainties, and extrapolation to the kinematics relevant for future colliders such as the LHC is an important challenge to high energy physics in recent years.

The PDF's are derived from global analysis of experimental data from a wide range of hard processes in the framework of perturbative QCD. In this work this important problem is studied with the help of the method of the structure function reconstruction over their Mellin moments, which is based on the expansion of the structure function in terms of Jacobi polynomials. This method was developed and applied for QCD analysis [6–16]. The same method has also been applied in a polarized case in Refs. [17] and [4,18–21].

In this paper we use the deep-inelastic world data for nonsinglet QCD analysis to obtain the parton distribution function up to next-to-next-to-leading order (NNLO) approximations. The results of the present analysis is based on the Jacobi polynomials expansion of the nonsinglet structure function.

The plan of the paper is to give an introduction of the Jacobi polynomials approach in Sec. II. The method of the QCD analysis of nonsinglet structure function, based on Jacobi polynomials, are written down in this section. In Sec. III we present a brief review of the theoretical formalism of the QCD analysis. A description of the procedure of the QCD fit of F_2 data are illustrated in Sec. IV. Section V contains final results of the QCD analysis. Our conclusions are summarized in Sec. VI.

II. JACOBI POLYNOMIALS APPROACH

The evolution equations allow one to calculate the Q^2 dependence of the parton distributions provided at a certain reference point Q_0^2. These distributions are usually parameterized on the basis of plausible theoretical assumptions concerning their behavior near the end points $x = 0, 1$.

One of the simplest and fastest possibilities in the structure function reconstruction from the QCD predictions for its Mellin moments is Jacobi polynomials expansion. The Jacobi polynomials are especially suitable for this purpose since they allow one to factor out an essential part of the x dependence of the structure function into the weight function [6]. Thus, given the Jacobi moments $a_n(Q^2)$, a structure function $f(x, Q^2)$ may be reconstructed in a form of

*Khorramiana@theory.ipm.ac.ir
URL: http://particles.ipm.ir/
+Atashbar@ipm.ir

the series [7–11]

$$xf(x,Q^2) = x^\beta(1-x)^\alpha \sum_{n=0}^{N_{\max}} a_n(Q^2)\Theta_n^{\alpha,\beta}(x), \quad (1)$$

where $N_{\max}$ is the number of polynomials and $\Theta_n^{\alpha,\beta}(x)$ are the Jacobi polynomials of order n,

$$\Theta_n^{\alpha,\beta}(x) = \sum_{j=0}^{n} c_j^{(n)}(\alpha,\beta)x^j, \quad (2)$$

where $c_j^{(n)}(\alpha,\beta)$ are the coefficients expressed through Γ functions and satisfy the orthogonality relation with the weight $x^\beta(1-x)^\alpha$ as in the following:

$$\int_0^1 dx x^\beta(1-x)^\alpha \Theta_k^{\alpha,\beta}(x)\Theta_l^{\alpha,\beta}(x) = \delta_{k,l}. \quad (3)$$

For the moment, we note that the Q^2 dependence is entirely contained in the Jacobi moments

$$\begin{aligned} a_n(Q^2) &= \int_0^1 dx x f(x,Q^2)\Theta_k^{\alpha,\beta}(x) \\ &= \sum_{j=0}^{n}\int_0^1 dx x^{j+1} c_j^{(n)}(\alpha,\beta) f(x,Q^2) \\ &= \sum_{j=0}^{n} c_j^{(n)}(\alpha,\beta) f(j+2,Q^2), \end{aligned} \quad (4)$$

obtained by inverting Eq. (1), using Eqs. (2) and (3) and also definition of moments, $f(j,Q^2) = \int_0^1 dx x^{j-1} f(x,Q^2)$.

Using Eqs. (1)–(4) now, one can relate the structure function with its Mellin moments

$$\begin{aligned} F_2^{N_{\max}}(x,Q^2) = x^\beta(1-x)^\alpha \sum_{n=0}^{N_{\max}} \Theta_n^{\alpha,\beta}(x) \\ \times \sum_{j=0}^{n} c_j^{(n)}(\alpha,\beta) F_2(j+2,Q^2), \end{aligned} \quad (5)$$

where $F_2(j+2,Q^2)$ are the moments determined in the next section. $N_{\max}$, α, and β have to be chosen so as to achieve the fastest convergence of the series on the right-hand side of Eq. (5) and to reconstruct xg_1 with the required accuracy. In our analysis we use $N_{\max} = 9$, $\alpha = 3.0$, and $\beta = 0.5$. The same method has been applied to calculate the nonsinglet structure function xF_3 from their moments [12–15] and for polarized structure function xg_1 [4,17,18].

Obviously the Q^2 dependence of the polarized structure function is defined by the Q^2 dependence of the moments.

III. THEORETICAL FORMALISM OF THE QCD ANALYSIS

In the common $\overline{\text{MS}}$ factorization scheme the relevant F_2 structure function as extracted from the DIS ep process can be, up to NNLO, written as [22–25]

$$F_2(x,Q^2) = F_{2,\text{NS}}(x,Q^2) + F_{2,S}(x,Q^2) + F_{2,g}(x,Q^2). \quad (6)$$

The nonsinglet structure function $F_{2,\text{NS}}(x,Q^2)$ for three active (light) flavors has the representation

$$\begin{aligned} \frac{1}{x}F_{2,\text{NS}}(x,Q^2) &= C_{2,\text{NS}}(x,Q^2) \otimes \left[\frac{1}{18}q_8^+ + \frac{1}{6}q_3^+\right](x,Q^2) \\ &= [C_{2,q}^{(0)} + aC_{2,\text{NS}}^{(1)} + a^2 C_{2,\text{NS}}^{(2)+}] \\ &\quad \otimes \left[\frac{1}{18}q_8^+ + \frac{1}{6}q_3^+\right](x,Q^2). \end{aligned} \quad (7)$$

The flavor singlet and gluon contributions in Eq. (6) reads

$$\begin{aligned} \frac{1}{x}F_{2,S}(x,Q^2) &= \frac{2}{9}C_{2,q} \otimes \Sigma(x,Q^2) \\ &= \frac{2}{9}[C_{2,q}^{(0)} + aC_{2,q}^{(1)} + a^2 C_{2,q}^{(2)}] \otimes \Sigma(x,Q^2); \end{aligned} \quad (8)$$

$$\begin{aligned} \frac{1}{x}F_{2,g}(x,Q^2) &= \frac{2}{9}C_{2,g} \otimes g(x,Q^2) \\ &= \frac{2}{9}[aC_{2,g}^{(1)} + a^2 C_{2,g}^{(2)}] \otimes g(x,Q^2). \end{aligned} \quad (9)$$

The symbol $\otimes$ denotes the Mellin convolution

$$[A \otimes B](x) = \int_0^1 dx_1 \int_0^1 dx_2 \delta(x - x_1x_2)A(x_1)B(x_2). \quad (10)$$

In Eq. (7) $q_3^+ = u + \bar{u} - (d + \bar{d}) = u_v - d_v$ and $q_8^+ = u + \bar{u} + d + \bar{d} - 2(s + \bar{s}) = u_v + d_v + 2\bar{u} + 2\bar{d} - 4\bar{s}$, where $s = \bar{s}$. Also in Eq. (8) $\Sigma(x,Q^2) \equiv \Sigma_{q=u,d,s}(q + \bar{q}) = u_v + d_v + 2\bar{u} + 2\bar{d} + 2\bar{s}$. Notice that in the above equations $a = a(Q^2) \equiv \alpha_s(Q^2)/4\pi$ denotes the strong coupling constant and $C_{i,j}(N)$ are the Wilson coefficients [26].

The combinations of parton densities in the nonsinglet regime and the valence region $x \geq 0.3$ for F_2^p in LO is

$$\frac{1}{x}F_2^p(x,Q^2) = \left[\frac{1}{18}q_{\text{NS},8}^+ + \frac{1}{6}q_{\text{NS},3}^+\right](x,Q^2) + \frac{2}{9}\Sigma(x,Q^2), \quad (11)$$

where $q_{\text{NS},3}^+ = u_v - d_v$, $q_{\text{NS},8}^+ = u_v + d_v$, and $\Sigma = u_v + d_v$, since sea quarks can be neglected in the region $x \geq 0.3$. So in the x space we have

$$\begin{aligned} F_2^p(x,Q^2) &= \left(\frac{5}{18}xq_{\text{NS},8}^+ + \frac{1}{6}xq_{\text{NS},3}^+\right)(x,Q^2) \\ &= \frac{4}{9}xu_v(x,Q^2) + \frac{1}{9}xd_v(x,Q^2). \end{aligned} \quad (12)$$

In the above region the combinations of parton densities for F_2^d are also given by

$$F_2^d(x,Q^2) = \left(\frac{5}{18}xq_{\rm NS,8}^+\right)(x,Q^2) = \frac{5}{18}x(u_v+d_v)(x,Q^2), \tag{13}$$

where $d = (p+n)/2$ and $q_{\rm NS,3}^+ = u_v - d_v$.

In the region $x \le 0.3$ for the difference of the proton and deuteron data we use

$$F_2^{\rm NS}(x,Q^2) \equiv 2(F_2^p - F_2^d)(x,Q^2) = \frac{1}{3}xq_{\rm NS,3}^+(x,Q^2) = \frac{1}{3}x(u_v-d_v)(x,Q^2) + \frac{2}{3}x(\bar{u}-\bar{d})(x,Q^2), \tag{14}$$

where now $q_{\rm NS,3}^+ = u_v - d_v + 2(\bar{u}-\bar{d})$ since sea quarks cannot be neglected for x smaller than about 0.3. In our calculation we supposed the $\bar{d}-\bar{u}$ distribution

$$x(\bar{d}-\bar{u})(x,Q_0^2) = 1.195x^{1.24}(1-x)^{9.10} \times (1 + 14.05x - 45.52x^2), \tag{15}$$

at $Q_0^2 = 4$ GeV^2 which gives a good description of the Drell–Yan dimuon production data [27]. In our analysis we used the above distribution for considering the symmetry breaking of sea quarks [28,29]. By using the solution of the nonsinglet evolution equation for the parton densities to 3-loop order [30], the nonsinglet structure functions are given by

$$F_2^k(N,Q^2) = (1 + aC_{2,\rm NS}^{(1)}(N) + a^2C_{2,\rm NS}^{(2)}(N))F_2^k(N,Q_0^2)\left(\frac{a}{a_0}\right)^{-\hat{P}_0(N)/\beta_0}\left\{1 - \frac{1}{\beta_0}(a-a_0)\left[\hat{P}_1^+(N) - \frac{\beta_1}{\beta_0}\hat{P}_0\right] - \frac{1}{2\beta_0}(a^2-a_0^2)\left[\hat{P}_2^+(N) - \frac{\beta_1}{\beta_0}\hat{P}_1^+ + \left(\frac{\beta_1^2}{\beta_0^2} - \frac{\beta_2}{\beta_0}\right)\hat{P}_0(N)\right] + \frac{1}{2\beta_0^2}(a-a_0)^2\left(\hat{P}_1^+(N) - \frac{\beta_1}{\beta_0}\hat{P}_0\right)^2\right\}. \tag{16}$$

Here $k = p$, d, and NS denotes the three above cases, i.e. proton, deuteron and nonsinglet structure function. $C_{2,\rm NS}^{(m)}(N)$ are the nonsinglet Wilson coefficients in $O(a_s^m)$ which can be found in [26,31,32] and $\hat{P}_m$ denote also the Mellin transforms of the $(m+1)$-loop splitting functions.

The strong coupling constant a_s plays a more central role in the present paper to the evolution of parton densities. At N^mLO the scale dependence of a_s is given by

$$\frac{da_s}{d\ln Q^2} = \beta_{N^mLO}(a_s) = -\sum_{k=0}^{m} a_s^{k+2}\beta_k. \tag{17}$$

The expansion coefficients β_k of the β function of QCD are known up to $k = 2$, i.e., N^{2}LO [33,34]

$$\beta_0 = 11 - 2/3n_f, \qquad \beta_1 = 102 - 38/3n_f, \qquad \beta_2 = 2857/2 - 5033/18n_f + 325/54n_f^2. \tag{18}$$

Here n_f stands for the number of effectively massless quark flavors. The strong coupling constant up to NNLO is as follows [35]:

$$a_s(Q^2) = \frac{1}{\beta_0 L_\Lambda} - \frac{1}{(\beta_0 L_\Lambda)^2}b_1 lnL_\Lambda + \frac{1}{(\beta_0 L_\Lambda)^3}[b_1^2(ln^2L_\Lambda - lnL_\Lambda - 1) + b_2], \tag{19}$$

where $L_\Lambda \equiv ln(Q^2/\Lambda^2)$, $b_k \equiv \beta_k/\beta_0$, and Λ is the QCD scale parameter.

IV. THE PROCEDURE OF THE QCD FITS OF F_2 DATA

In the present analysis we choose the following parametrization for the valence quark densities:

$$xu_v(x,Q_0^2) = \mathcal{N}_u x^{a_u}(1-x)^{b_u}(1 + c_u\sqrt{x} + d_u x),$$
$$xd_v(x,Q_0^2) = \mathcal{N}_d x^{a_d}(1-x)^{b_d}(1 + c_d\sqrt{x} + d_d x), \tag{20}$$

in the input scale of $Q_0^2 = 4$ GeV^2 and the normalizations $\mathcal{N}_u$ and $\mathcal{N}_d$ being fixed by $\int_0^1 u_v dx = 2$ and $\int_0^1 d_v dx = 1$, respectively. By QCD fits of the world data for $F_2^{p,d}$, we can extract valence quark densities using the Jacobi polynomials method. For the nonsinglet QCD analysis presented in this paper we use the structure function data measured in charged lepton proton and deuteron deep-inelastic scattering. The experiments contributing to the statistics are BCDMS [36], SLAC [37], NMC [38], H1 [39], and ZEUS [40]. In our QCD analysis we use three data samples: $F_2^p(x,Q^2)$, $F_2^d(x,Q^2)$ in the nonsinglet regime and the valence quark region $x \ge 0.3$ and $F_2^{\rm NS} = 2(F_2^p - F_2^d)$ in the region $x < 0.3$.

The valence quark region may be parameterized by the nonsinglet combinations of parton distributions, which are expressed through the parton distributions of valence quarks. Only data with $Q^2 > 4$ GeV^2 were included in the analysis and a cut in the hadronic mass of $W^2 \equiv (\frac{1}{x} - 1)Q^2 + m_N^2 > 12.5$ GeV^2 was applied in order to widely eliminate higher twist (HT) effects from the data samples. After these cuts we are left with 762 data points, 322 for F_2^p, 232 for F_2^d, and 208 for $F_2^{\rm NS}$. By considering the additional cuts on the BCDMS ($y > 0.35$) and on the

NMC data ($Q^2 > 8$ GeV^2) the total number of data points available for the analysis reduce from 762 to 551.

The simplest possible choice for the χ^2 function would be

$$\chi^2 = \sum_{i=1}^{n^{\text{data}}} \frac{(F_{2,i}^{\text{data}} - F_{2,i}^{\text{theor}})^2}{(\Delta F_{2,i}^{\text{data}})^2}, \tag{21}$$

where $\Delta F_{2,i}^{\text{data}}$ is the error associated with data point i. Through $F_{2,i}^{\text{theor}}$, χ^2 is a function of the theory parameters. Minimization of χ^2 would identify parameter values for which the theory fits the data. However, the simple form is appropriate only for the ideal case of a uniform data set with uncorrelated errors. For data used in the global analysis, most experiments combine various systematic errors into one effective error for each data point, along with the statistical error. Then, in addition, the fully correlated normalization error of the experiment is usually specified separately. For this reason, it is natural to adopt the following definition for the effective χ^2 [41]:

$$\chi^2_{\text{global}} = \sum_n w_n \chi^2_n \quad (n \text{ labels the different experiments}), \tag{22}$$

$$\chi^2_n = \left(\frac{1 - \mathcal{N}_n}{\Delta \mathcal{N}_n}\right)^2 + \sum_i \left(\frac{\mathcal{N}_n F_{2,i}^{\text{data}} - F_{2,i}^{\text{theor}}}{\mathcal{N}_n \Delta F_{2,i}^{\text{data}}}\right)^2. \tag{23}$$

For the nth experiment, $F_{2,i}^{\text{data}}$, $\Delta F_{2,i}^{\text{data}}$, and $F_{2,i}^{\text{theor}}$ denote the data value, measurement uncertainty (statistical and systematic combined), and theoretical value for the ith data point. $\Delta \mathcal{N}_n$ is the experimental normalization uncer-

TABLE I. Number of experimental data points (a) F_2^p, (b) F_2^d, and (c) F_2^{NS} for the nonsinglet QCD analysis with their x and Q^2 ranges. The name of different data sets and range of x and Q^2 are given in the three first columns. The fourth column (F_2) contains the number of data points according to the cuts: $Q^2 > 4$ GeV^2, $W^2 > 12.5$ GeV^2, $x > 0.3$ for F_2^p and F_2^d and $x < 0.3$ for F_2^{NS}. The reduction of the number of data points by the additional cuts (see text) are given in the fifthth column (F_2 cuts). The normalization shifts are listed in the last column.

(a) Number of F_2^p data points.

Experiment	x	Q^2, GeV^2	F_2^p	F_2^p cuts	$\mathcal{N}$
BCDMS (100)	0.35–0.75	11.75–75.00	51	29	1.005
BCDMS (120)	0.35–0.75	13.25–75.00	59	32	0.998
BCDMS (200)	0.35–0.75	32.50–137.50	50	28	0.998
BCDMS (280)	0.35–0.75	43.00–230.00	49	26	0.998
NMC (comb)	0.35–0.50	7.00–65.00	15	14	1.000
SLAC (comb)	0.30–0.62	7.30–21.39	57	57	1.013
H1 (hQ2)	0.40–0.65	200–30000	26	26	1.020
ZEUS (hQ2)	0.40–0.65	650–30000	15	15	1.007
proton			322	227	

(b) Number of F_2^d data points.

Experiment	x	Q^2, GeV^2	F_2^d	F_2^d cuts	$\mathcal{N}$
BCDMS (120)	0.35–0.75	13.25–99.00	59	32	1.001
BCDMS (200)	0.35–0.75	32.50–137.50	50	28	0.998
BCDMS (280)	0.35–0.75	43.00–230.00	49	26	1.003
NMC (comb)	0.35–0.50	7.00–65.00	15	14	1.000
SLAC (comb)	0.30–0.62	10.00–21.40	59	59	0.990
deuteron			232	159	

(c) Number of F_2^{NS} data points.

Experiment	x	Q^2, GeV^2	F_2^{NS}	F_2^{NS} cuts	$\mathcal{N}$
BCDMS (120)	0.070–0.275	8.75–43.00	36	30	0.983
BCDMS (200)	0.070–0.275	17.00–75.00	29	28	0.999
BCDMS (280)	0.100–0.275	32.50–115.50	27	26	0.997
NMC (comb)	0.013–0.275	4.50–65.00	88	53	1.000
SLAC (comb)	0.153–0.293	4.18–5.50	28	28	0.994
nonsinglet			208	165	

tainty and $\mathcal{N}_n$ is an overall normalization factor for the data of experiment n. The factor w_n is a possible weighting factor (with default value 1). However, we allowed for a relative normalization shift $\mathcal{N}_n$ between the different data sets within the normalization uncertainties $\Delta\mathcal{N}_n$ quoted by the experiments. For example the normalization uncertainty of the NMC (combined) data is estimated to be 2.5%. The normalization shifts $\mathcal{N}_n$ were fitted once and then kept fixed.

The number of data points for the nonsinglet QCD analysis with their x and Q^2 ranges and the normalization shifts determined are summarized in Table I. In this table the first column gives (in parentheses) the beam momentum in GeV of the respective data set (number), a flag whether the data come from a combined analysis of all beam momenta (comb) or whether the data are taken at high momentum transfer (hQ2). The x and Q^2 range indicate in the second and third columns, respectively. The fourth column (F_2) contains the number of data points according to the cuts: $Q^2 > 4$ GeV^2, $W^2 > 12.5$ GeV^2, $x > 0.3$ for F_2^p and F_2^d and $x < 0.3$ for $F_2^{\rm NS}$. The reduction of the number of data points by the additional cuts on the BCDMS data ($y > 0.3$) and on the NMC data ($Q^2 > 8$ GeV^2) are given in the fifth column (F_2 cuts). The last column ($\mathcal{N}$) contains the normalization shifts.

Now the sums in $\chi^2_{\rm global}$ run over all data sets and in each data set over all data points. The minimization of the above χ^2 value to determine the best parametrization of the unpolarized parton distributions is done using the program MINUIT [42].

The one σ error for the parton density f_q as given by Gaussian error propagation is [30]

$$\sigma(f_q(x))^2 = \sum_{i=1}^{n_p}\sum_{j=1}^{n_p}\left(\frac{\partial f_q}{\partial p_i}\right)\left(\frac{\partial f_q}{\partial p_j}\right)\mathrm{cov}(p_i, p_j), \qquad (24)$$

where the sum runs over all fitted parameters. The functions $\partial f_q/\partial p_i$ are the derivatives of f_q with respect to the fit parameter p_i, and $\mathrm{cov}(p_i, p_j)$ are the elements of the covariance matrix. The derivatives $\partial f_q/\partial p_i$ can be calculated analytically at the input scale Q_0^2. Their values at Q^2 are given by evolution which is performed in Mellin–N space.

V. RESULTS

In the QCD analysis of the present paper we used three data sets: the structure functions $F_2^p(x, Q^2)$ and $F_2^d(x, Q^2)$ in the region of $x \geq 0.3$ and the combination of these structure functions $F_2^{\rm NS}(x, Q^2)$ in the region of $x < 0.3$. Notice that we take into account the cuts $Q^2 > 4$ GeV^2, $W^2 > 12.5$ GeV^2 for our QCD fits to determine some unknown parameters. In Fig. 1 the proton data for $F_2(x, Q^2)$ are shown in the nonsinglet regime and the valence quark region $x \geq 0.3$ indicating the above cuts

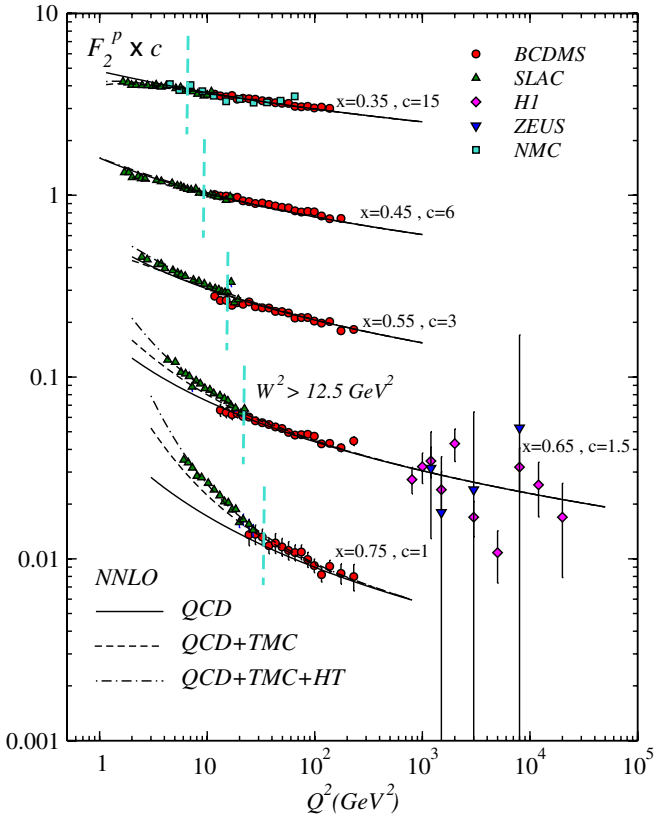

FIG. 1 (color online). The structure function F_2^p as a function of Q^2 in intervals of x. Shown are the pure QCD fit in NNLO (solid line) and the contributions from target mass corrections (dashed line) and higher twist (dashed-dotted line). The vertical dashed line indicates the regions with $W^2 > 12.5$ GeV^2.

by a vertical dashed line. The solid lines correspond to the NNLO QCD fit.

Now it is possible to take into account the target mass effects in our calculations. The perturbative form of the moments is derived under the assumption that the mass of the target hadron is zero (in the limit $Q^2 \to \infty$). At intermediate and low Q^2 this assumption will begin to break down and the moments will be subject to potentially significant power corrections, of order $\mathcal{O}(m_N^2/Q^2)$, where m_N is the mass of the nucleon. These are known as target mass corrections (TMCs) and when included, the moments of flavor nonsinglet structure function have the form [43,44]

$$\begin{aligned} F_{2,\rm TMC}^k(n, Q^2) &\equiv \int_0^1 x^{n-2} F_{2,\rm TMC}^k(x, Q^2)dx \\ &= F_2^k(n, Q^2) + \frac{n(n-1)}{n+2}\left(\frac{m_N^2}{Q^2}\right)F_2^k(n+2, Q^2) \\ &\quad + \frac{(n+2)(n+1)n(n-1)}{2(n+4)(n+3)}\left(\frac{m_N^2}{Q^2}\right)^2 \\ &\quad \times F_2^k(n+4, Q^2) + \mathcal{O}\left(\frac{m_N^2}{Q^2}\right)^3, \end{aligned} \qquad (25)$$

where higher powers than $(m_N^2/Q^2)^2$ are negligible for the

relevant $x < 0.8$ region. By inserting Eq. (25) in Eq. (5) we have

$$F_2^{N_{\max},k}(x, Q^2) = x^\beta (1-x)^\alpha \sum_{n=0}^{N_{\max}} \Theta_n^{\alpha,\beta}(x) \times \sum_{j=0}^{n} c_j^{(n)}(\alpha, \beta) F_{2,\mathrm{TMC}}^k(j+2, Q^2), \quad (26)$$

where $F_{2,\mathrm{TMC}}^k(j+2, Q^2)$ are the moments determined by Eq. (25). In Fig. 1 the dashed lines correspond to the NNLO QCD fit adding target mass corrections.

Despite the kinematic cuts [$Q^2 \geq 4$ GeV^2, $W^2 \equiv (\frac{1}{x} - 1)Q^2 + m_N^2 \geq 12.5$ GeV^2] used for our analysis, we also take into account higher twist corrections to $F_2^p(x, Q^2)$ and $F_2^d(x, Q^2)$ in the kinematic region $Q^2 \geq 4$ GeV^2, $4 < W^2 < 12.5$ GeV^2 in order to learn whether nonperturbative effects may still contaminate our perturbative analysis. For this purpose we extrapolate the QCD fit results obtained for $W^2 \geq 12.5$ GeV^2 to the region $Q^2 \geq 4$ GeV^2, $4 < W^2 < 12.5$ GeV^2 and form the difference between data and theory, applying target mass corrections in addition. Now by considering higher twist correction (HT)

$$F_2^{\exp}(x, Q^2) = O_{\mathrm{TMC}}[F_2^{\mathrm{HT}}(x, Q^2)] \cdot \left(1 + \frac{h(x, Q^2)}{Q^2\ [\mathrm{GeV}^2]}\right), \quad (27)$$

the higher twist coefficient can be extract. Here the operation $O_{\mathrm{TMC}}[\ldots]$ denotes taking the target mass corrections of the twist-2 contributions to the respective structure function. The coefficients $h(x, Q^2)$ are determined in bins of x and Q^2 and are then averaged over Q^2. We extrapolate our QCD fits to the region 12.5 GeV$^2 \geq W^2 \geq 4$ GeV^2 in Fig. 1. The dashed-dotted lines in this figure correspond to the NNLO QCD fit adding target mass and higher twist corrections. There, at higher values of x a clear gap between the data and the QCD fit is seen. Fig. 2 shows the corresponding results for the deuteron data. Figure 3 shows the result of the pure QCD fit for the nonsinglet structure function in NNLO.

In Table II we summarize the LO, NLO, and NNLO fit results without HT contributions for the parameters of the parton densities $xu_v(x, Q_0^2)$, $xd_v(x, Q_0^2)$, and $\Lambda_{\mathrm{QCD}}^{N_f=4}$. The resulted value of χ^2/ndf is 0.9853 at LO, 0.9578 at NLO, and 0.9267 at NNLO. Our results for covariance matrix for LO, NLO, and NNLO are presented in Table III.

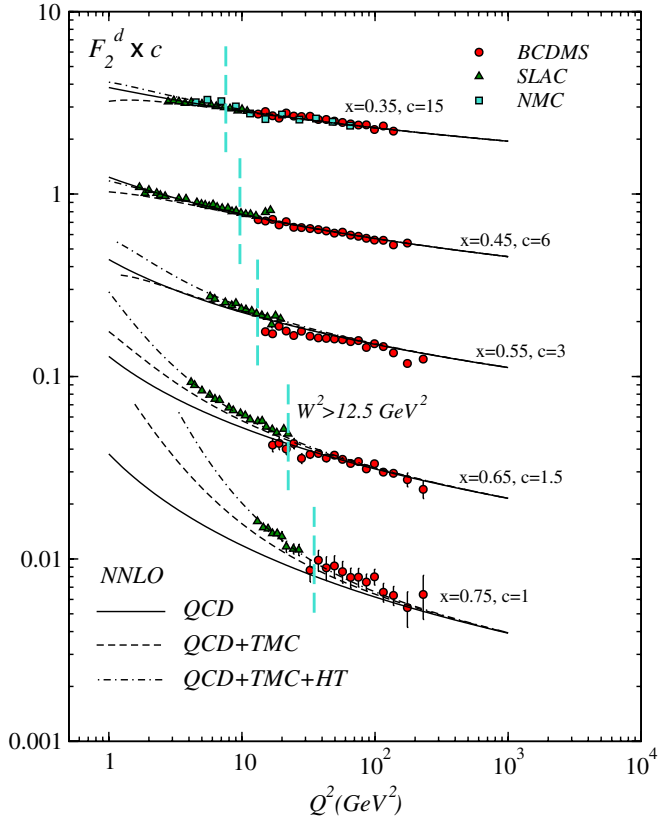

FIG. 2 (color online). The structure function F_2^d as a function of Q^2 in intervals of x. Shown are the pure QCD fit in NNLO (solid line) and the contributions from target mass corrections (dashed line) and higher twist (dashed-dotted line). The vertical dashed lines indicate the regions with $W^2 > 12.5$ GeV^2.

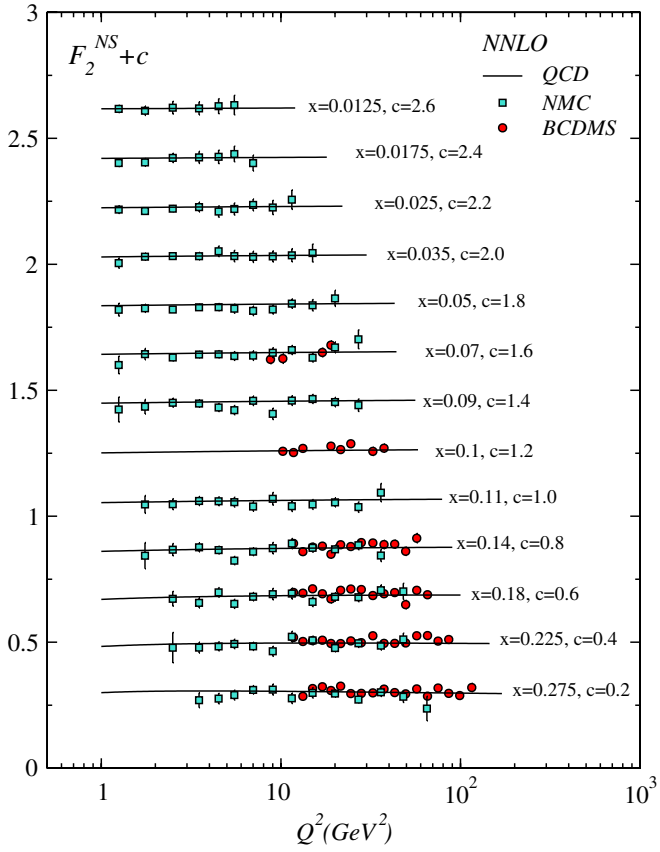

FIG. 3 (color online). The structure function F_2^{NS} as a function of Q^2 in intervals of x. Shown is the pure QCD fit in NNLO (solid lines).

TABLE II. Parameter values of the LO, NLO, and NNLO nonsinglet QCD fit at $Q_0^2 = 4$ GeV^2. The values without error have been fixed after a first minimization since the data do not constrain these parameters well enough (see text).

		LO	NLO	NNLO
u_v	a_u	0.6698 ± 0.0073	0.7434 ± 0.009	0.7772 ± 0.009
	b_u	3.5104 ± 0.042	3.8907 ± 0.040	4.0034 ± 0.033
	c_u	0.1990	0.1620	0.1000
	d_u	1.498	1.2100	1.1400
d_v	a_d	0.6850 ± 0.035	0.7369 ± 0.040	0.7858 ± 0.043
	b_d	3.1685 ± 0.192	3.5051 ± 0.225	3.6336 ± 0.244
	c_d	0.5399	0.3899	0.1838
	d_d	-1.4000	-1.3700	-1.2152
$\Lambda_{\rm QCD}^{\rm N_f=4}$, MeV		213.2 ± 28	263.8 ± 30	239.9 ± 27
χ^2/ndf		$538/546 = 0.9853$	$523/546 = 0.9578$	$506/546 = 0.9267$

Figure 4 illustrates our fit results for $xu_v(x, Q_0^2)$, $xd_v(x, Q_0^2)$ at $Q_0^2 = 4$ GeV^2 at NNLO with correlated errors. We compare with the results of [30,44,45] and a very recent analysis [46]. Our results for $xu_v(x, Q_0^2)$ and $xd_v(x, Q_0^2)$ are in good agreement with the other theoretical model at the one σ level.

In Figs. 5 and 6 we show the evolution of the valence quark distributions $xu_v(x, Q^2)$ and $xd_v(x, Q^2)$ from $Q^2 = 10$ GeV^2 to $Q^2 = 10^4$ GeV^2 in the region $x \in [10^{-4}, 1]$ up to NNLO. We also compared with other QCD analysis [30,45–47]. With rising values of Q^2 the distributions flatten at large values of x and rise at low values.

Another way to compare the NNLO fit results consists in forming moments of the distributions $u_v(x, Q^2)$, $d_v(x, Q^2)$. In Table IV we present the lowest nontrivial moments of these distributions at $Q^2 = Q_0^2$ in NNLO and compare to the respective moments obtained for the parameterizations [30,47–49].

To perform higher twist QCD analysis of the nonsinglet world data up to NNLO, we consider the $Q^2 \geq 4$ GeV^2, $4 < W^2 < 12.5$ GeV^2 cuts. The number of data points in the above range for proton and deuteron is 279 and 278, respectively. The extracted distributions for $h(x)$ up to NNLO are depicted in Fig. 7 for the nonsinglet case con-

TABLE III. Our results for the covariance matrix of the LO, NLO, and NNLO nonsinglet QCD fit at $Q_0^2 = 4$ GeV^2 by using MINUIT [42].

LO	a_u	b_u	a_d	b_d	$\Lambda_{\rm QCD}^{\rm N_f=4}$
a_u	$\mathbf{5.28 \times 10 - 5}$				
b_u	$1.65 \times 10 - 4$	$\mathbf{1.73 \times 10 - 3}$			
a_d	$-7.39 \times 10 - 5$	$-4.55 \times 10 - 4$	$\mathbf{1.23 \times 10 - 3}$		
b_d	$-2.64 \times 10 - 4$	$-2.12 \times 10 - 3$	$6.15 \times 10 - 3$	$\mathbf{3.67 \times 10 - 2}$	
$\Lambda_{\rm QCD}^{(4)}$	$1.90 \times 10 - 5$	$-8.34 \times 10 - 4$	$2.39 \times 10 - 5$	$-3.16 \times 10 - 4$	$\mathbf{7.79 \times 10 - 4}$

NLO	a_u	b_u	a_d	b_d	$\Lambda_{\rm QCD}^{\rm N_f=4}$
a_u	$\mathbf{8.87 \times 10 - 5}$				
b_u	$2.39 \times 10 - 4$	$\mathbf{1.63 \times 10 - 3}$			
a_d	$-1.34 \times 10 - 4$	$-7.86 \times 10 - 4$	$\mathbf{1.61 \times 10 - 3}$		
b_d	$-5.10 \times 10 - 4$	$-4.19 \times 10 - 3$	$8.33 \times 10 - 3$	$\mathbf{5.07 \times 10 - 2}$	
$\Lambda_{\rm QCD}^{(4)}$	$8.71 \times 10 - 5$	$-5.39 \times 10 - 4$	$8.09 \times 10 - 5$	$2.57 \times 10 - 4$	$\mathbf{8.80 \times 10 - 4}$

NNLO	a_u	b_u	a_d	b_d	$\Lambda_{\rm QCD}^{\rm N_f=4}$
a_u	$\mathbf{7.61 \times 10 - 5}$				
b_u	$1.73 \times 10 - 4$	$\mathbf{1.10 \times 10 - 3}$			
a_d	$-8.41 \times 10 - 5$	$-6.62 \times 10 - 4$	$\mathbf{1.85 \times 10 - 3}$		
b_d	$-2.73 \times 10 - 4$	$-3.73 \times 10 - 3$	$9.79 \times 10 - 3$	$\mathbf{5.98 \times 10 - 2}$	
$\Lambda_{\rm QCD}^{(4)}$	$1.08 \times 10 - 4$	$-2.74 \times 10 - 4$	$1.06 \times 10 - 4$	$4.19 \times 10 - 4$	$\mathbf{7.41 \times 10 - 4}$

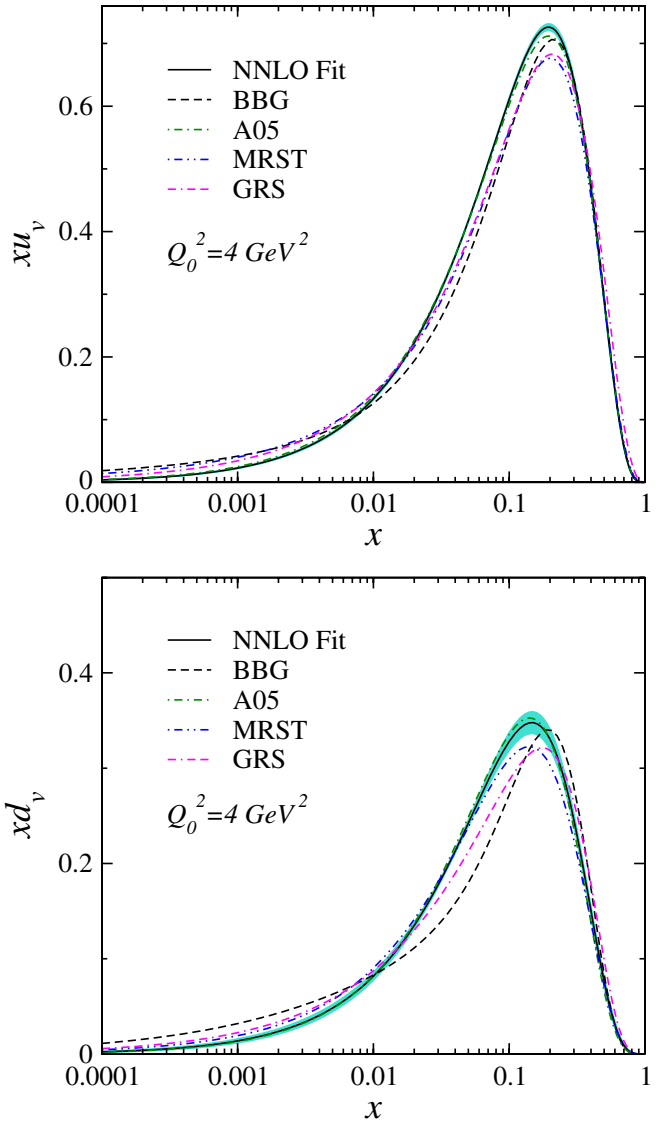

FIG. 4 (color online). The parton densities xu_v and xd_v at the input scale $Q_0^2 = 4.0$ GeV^2 (solid line) compared to results obtained from NNLO analysis by BBG (dashed-line) [30], A05 (dashed-dotted line) [45], MRST (dashed-dotted-dotted line) [46], and GRS (dashed-dashed-dotted line) [44]. The shaded areas represent the fully correlated one σ statistical error bands.

sidering scattering off the proton target. According to our results the coefficient $h(x)$ grows towards large x. Also in this figure HT contributions have the tendency to decrease form LO to NLO, NNLO. This effect was observed for the first time in the case of fits of F_3 DIS νN data in [12] and then studied in more detail in [14,15].

This similar effect was also observed in the fits of F_2 charge lepton-nucleon DIS data [30,44,50,51]. To compare, we also present the reported results of the early NNLO analysis [44,51] in Fig. 7. Note that the results for $h(x)$ in LO are not presented in the BBG model [30,51]. In Ref. [44], the functional form for $h(x)$ is chosen by

$$h(x) = a\left(\frac{x^b}{1-x} - c\right), \tag{28}$$

and it is possible to compare $h(x)$ results even in LO. Figure 8 shows our results for $h(x)$ and for the deuteron target up to NNLO. Also we compare the results for the BBG model [51]. The same as the proton, HT contributions for the deuteron have the tendency to decrease form LO to NLO, NNLO. As seen from Figs. 7 and 8 $h(x)$ is widely independent of the target comparing the results for deeply inelastic scattering off protons and deuterons. Our results in low-x are also in good agreement with [30,51].

VI. DISCUSSION

We have performed a QCD analysis of the flavor nonsinglet unpolarized deep-inelastic charged lepton-nucleon scattering data to next-to-leading order and derived parameterizations of valence quark distributions at a starting scale Q_0^2 together with the QCD scale $\Lambda_{\rm QCD}$ by using the Jacobi polynomial expansions.

The analysis was performed using the Jacobi polynomials method to determine the parameters of the problem in a fit to the data. A new aspect in comparison with previous analysis is that we determine the parton densities and the QCD scale up to NNLO by using the Jacobi polynomial expansion method. The benefit of this approach is the possibility to determine nonsinglet parton distributions analytically and not numerically. In Ref. [52] we arrange the MATHEMATICA program to extract $xu_v(x, Q^2)$ and $xd_v(x, Q^2)$.

In this paper the flavor asymmetric combination of light parton distributions $x(\bar{d} - \bar{u})$ of Eq. (15) are fixed at $Q_0^2 = 4$ GeV^2, as GRS [44] and BBG [29,30] applied, and gives a good description of the Drell-Yan dimuon production data [53]. The first clear evidence for the flavor asymmetry of the nucleon sea in nature came from the analysis of NMC at CERN [54]. In order to have the link with NMC data, we want to study the compatibility of the $x(\bar{d} - \bar{u})$ with the NMC result for the Gottfried sum rule (GSR) [55]. This sum rule is still actively discussed in problems of deep-inelastic scattering. The GSR, $I_{\rm GSR}$, can be expressed in terms of the parton distribution functions as

$$\begin{aligned} I_{\rm GSR}(Q^2) &\equiv \int_0^1 [F_2^{lp}(x, Q^2) - F_2^{ln}(x, Q^2)]\frac{dx}{x} \\ &= \int_0^1 \Big[\frac{1}{3}(u_v(x, Q^2) - d_v(x, Q^2)) \\ &\quad + \frac{2}{3}(\bar{u}(x, Q^2) - \bar{d}(x, Q^2))\Big]dx \\ &= \frac{1}{3} + \frac{2}{3}\int_0^1 (\bar{u}(x, Q^2) - \bar{d}(x, Q^2))dx. \end{aligned} \tag{29}$$

In the derivation of the above equation, the asymmetry of nucleon sea was assumed. The NMC measurement [54]

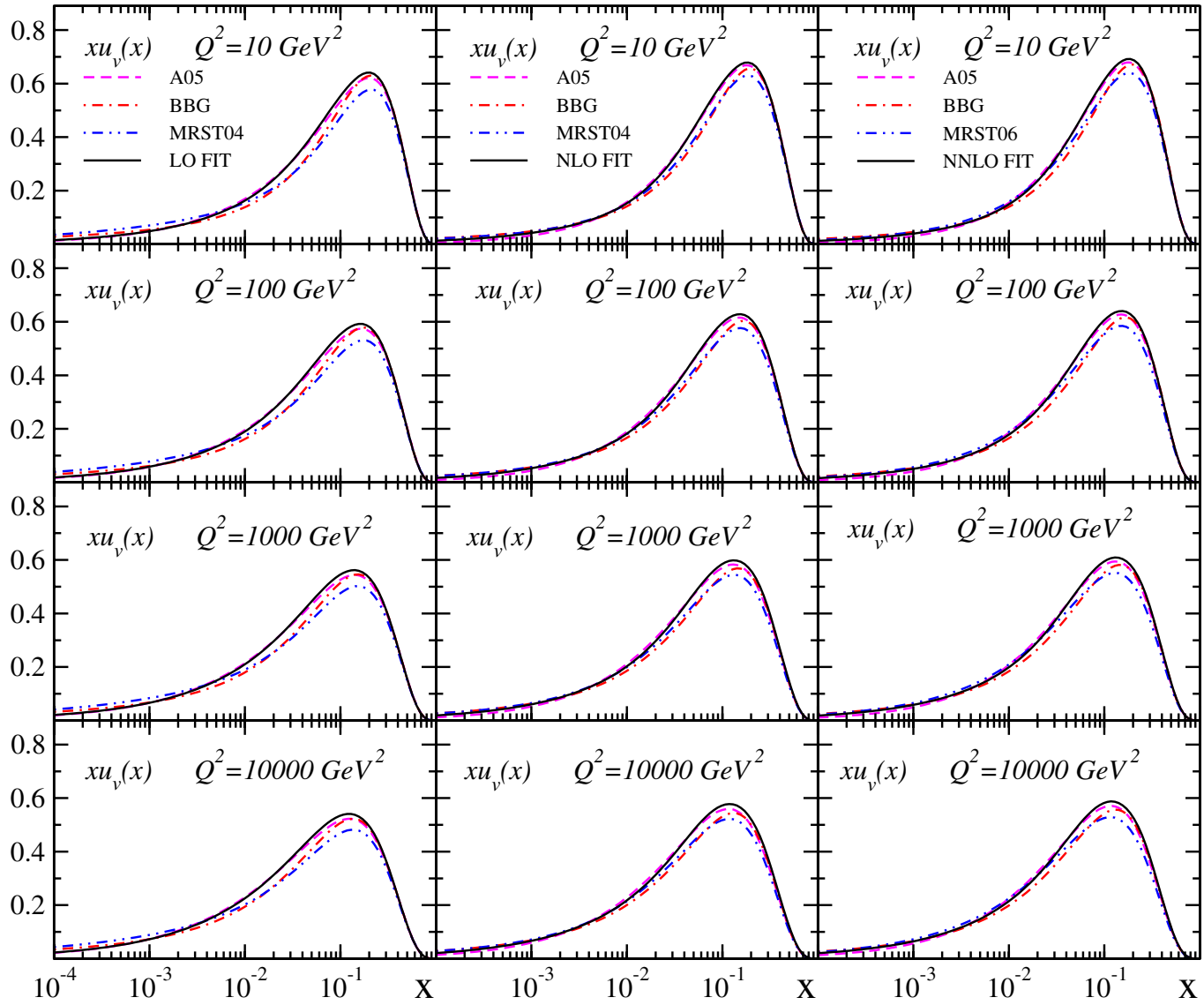

FIG. 5 (color online). The parton density xu_v at NNLO evolved up to $Q^2 = 10,000$ GeV^2 (solid lines) compared with results obtained by A05 (dashed line) [45], BBG (dashed-dotted line) [30], and MRST (dashed-dotted-dotted line) [46,47].

implies at $Q^2 = 4$ GeV^2

$$\int_0^1 (\bar{d}(x, Q^2) - \bar{u}(x, Q^2))dx = 0.148 \pm 0.039, \qquad (30)$$

which was the first indication that there are more down antiquarks in the proton than up antiquarks. On the other hand, this value is reported 0.118 ± 0.012 at $Q^2 = 54$ GeV^2 [27]. Now it is interesting to obtain this value for the parametrization of Eq. (15) which we used in our QCD analysis. By integration of this distribution we obtain $\simeq 0.1$ which is smaller than the reported results in the literature. However, the NMC Collaboration gives the $I_{\rm GSR}$ experimental value at $Q^2 = 4$ GeV^2 [54]

$$I^{\rm exp}_{\rm GSR}(Q^2 = 4\ {\rm GeV}^2) = 0.235 \pm 0.026. \qquad (31)$$

By using Eq. (29) we obtain the GSR value of about 0.267 with which the existing measurements are almost compatible within error. It seems that although the value of $\int_0^1(\bar{d} - \bar{u})dx$ is smaller than the values in the literature, the parametrization of Eq. (15) can give a good description of the E866 experimental data [27]. Also we should notice that the GSR does not belong to the strict sum rules in QCD and it is necessary to receive not only QCD corrections but anomalous dimensions as well [56–61].

Now it is interesting to compare the NNLO theoretical QCD theoretical prediction for the Gottfried sum rule [58] with NMC data. The recent step in this direction was done

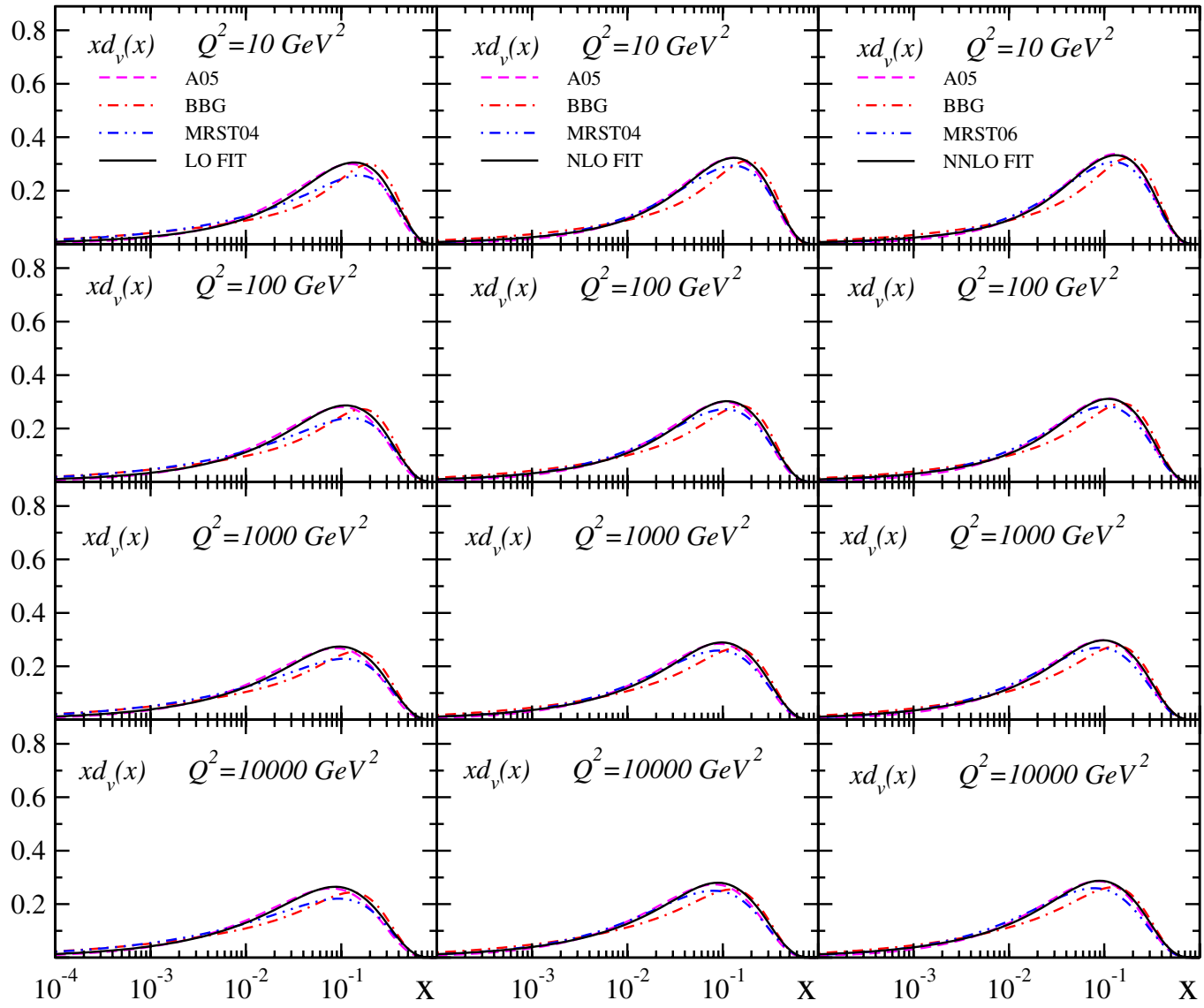

FIG. 6 (color online). The parton density xd_v at NNLO evolved up to $Q^2 = 10\,000$ GeV^2 (solid lines) compared to results obtained by A05 (dashed line) [45], BBG (dashed-dotted line) [30], and MRST (dashed-dotted-dotted line) [46,47].

in [62]. According to this paper we add the QCD two-loop correction to the Gottfried sum rule and we refine the GSR value to about 0.12%. Also we obtain the value of $I_{\rm GSR}(0.004 < x < 0.8, 4\ {\rm GeV}^2) = 0.267$ which is well compatible with the neural parametrization results, e.g. 0.2281 ± 0.0437 [62] within errors.

In the QCD analysis we parameterized the strong coupling constant α_s in terms of four massless flavors determining $\Lambda_{\rm QCD}$. The LO, NLO, and NNLO results fitting the

TABLE IV. Comparison of low order moments from our nonsinglet NNLO QCD analysis at $Q_0^2 = 4$ GeV^2 with the NNLO analysis BBG [30], MRST04 [47], A02 [48], and A06 [49].

f	N	NNLO	BBG	MRST04	A02	A06
u_v	2	0.3056 ± 0.0023	0.2986 ± 0.0029	0.285	0.304	0.2947
	3	0.0871 ± 0.0009	0.0871 ± 0.0011	0.082	0.087	0.0843
	4	0.0330 ± 0.0004	0.0333 ± 0.0005	0.032	0.033	0.0319
d_v	2	0.1235 ± 0.0023	0.1239 ± 0.0026	0.115	0.120	0.1129
	3	0.0298 ± 0.0008	0.0315 ± 0.0008	0.028	0.028	0.0275
	4	0.0098 ± 0.0004	0.0105 ± 0.0004	0.009	0.010	0.0092

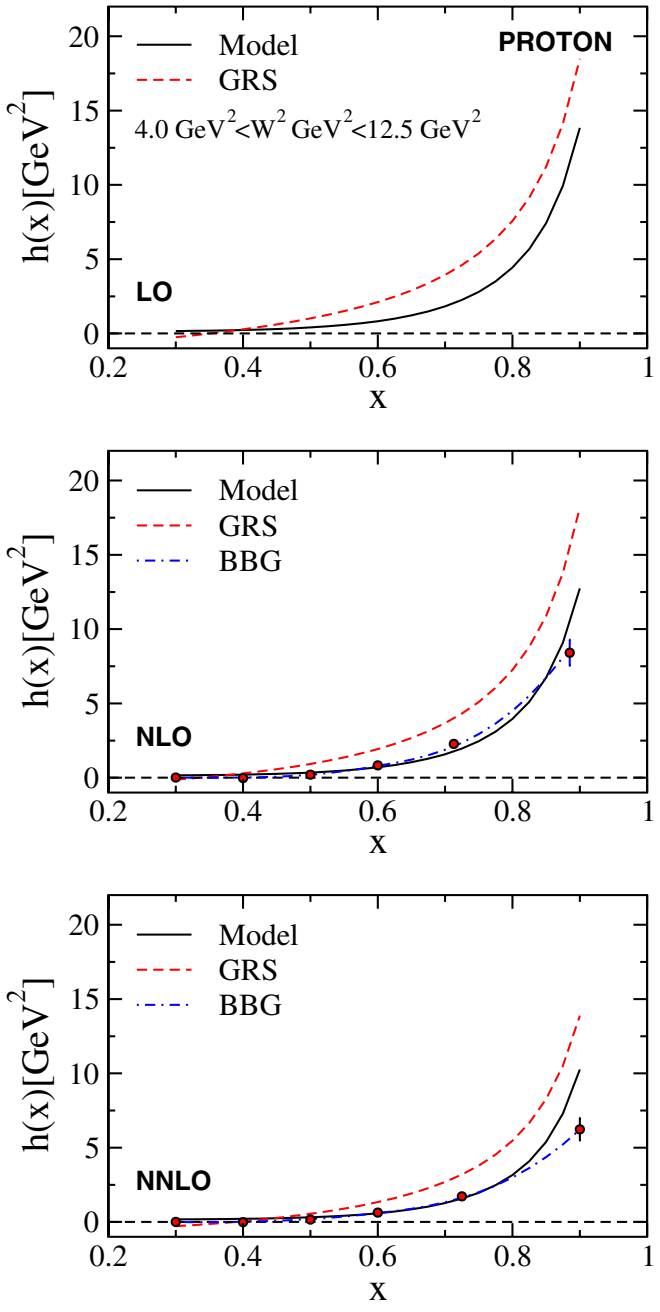

FIG. 7 (color online). The higher twist coefficient $h(x)$ for the proton data as a function of x up to NNLO (solid line) compared with results obtained by GRS (dashed line) [44] and BBG (dashed-dotted line) [51].

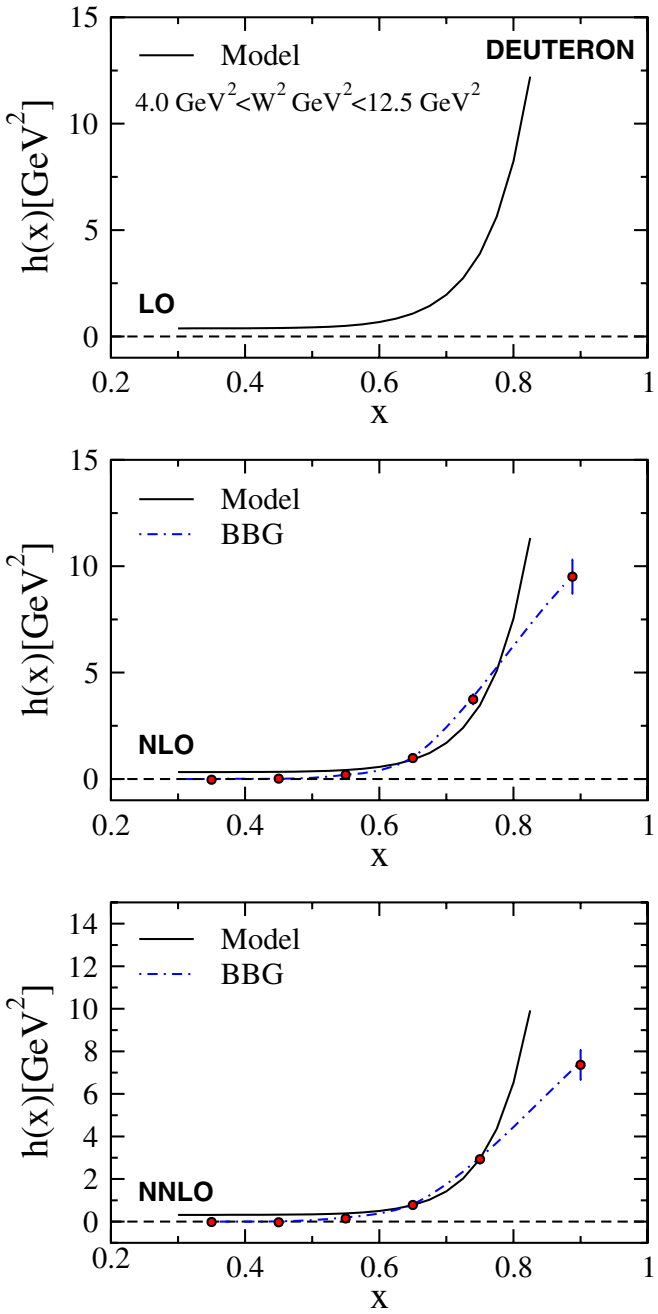

FIG. 8 (color online). The higher twist coefficient $h(x)$ for the deuteron data as a function of x up to NNLO (solid line) compared with results obtained by BBG (dashed-dotted line) [51].

data are

$$\begin{aligned}
\Lambda^{(4)\overline{\mathrm{MS}}}_{\mathrm{QCD}} &= 213.2 \pm 28 \text{ MeV}, \quad \text{LO}, \\
\Lambda^{(4)\overline{\mathrm{MS}}}_{\mathrm{QCD}} &= 263.8 \pm 30 \text{ MeV}, \quad \text{NLO}, \\
\Lambda^{(4)\overline{\mathrm{MS}}}_{\mathrm{QCD}} &= 239.9 \pm 27 \text{ MeV}, \quad \text{NNLO},
\end{aligned} \tag{32}$$

These results can be expressed in terms of $\alpha_s(M_Z^2)$:

$$\begin{aligned}
\alpha_s(M_Z^2) &= 0.1281 \pm 0.0028, \quad \text{LO}, \\
\alpha_s(M_Z^2) &= 0.1149 \pm 0.0021, \quad \text{NLO}, \\
\alpha_s(M_Z^2) &= 0.1131 \pm 0.0019, \quad \text{NNLO}.
\end{aligned} \tag{33}$$

Note that in above results we use the matching between n_f and n_{f+1} flavor couplings calculated in Ref. [63]. To be capable to compare with other measurement of Λ_{QCD} we adopt this prescription.

The $\alpha_s(M_Z^2)$ values can be compared with results from other QCD analysis of inclusive deep–inelastic scattering data in NLO

A02 [48] $\alpha_s(M_Z^2) = 0.1171 \pm 0.0015$,
ZEUS [64] $\alpha_s(M_Z^2) = 0.1166 \pm 0.0049$,
H1 [39] $\alpha_s(M_Z^2) = 0.1150 \pm 0.0017$,
BCDMS [36] $\alpha_s(M_Z^2) = 0.110 \pm 0.006$,
GRS [44] $\alpha_s(M_Z^2) = 0.112$,
CTEQ6 [65] $\alpha_s(M_Z^2) = 0.1165 \pm 0.0065$,
MRST03 [66] $\alpha_s(M_Z^2) = 0.1165 \pm 0.0020$,
BBG [30] $\alpha_s(M_Z^2) = 0.1148 \pm 0.0019$,
KK05 [67] $\alpha_s(M_Z^2) = 0.1153 \pm 0.0013(\text{stat}) \pm 0.0022(\text{syst}) \pm 0.0012(\text{norm})$,
BB(pol) [68] $\alpha_s(M_Z^2) = 0.113 \pm 0.004$,
AK(pol) [4] $\alpha_s(M_Z^2) = 0.1141 \pm 0.0036$.

The NNLO values of $\alpha_s(M_Z^2)$ can also be compared with results from other QCD analysis:

A02 [48] $\alpha_s(M_Z^2) = 0.1143 \pm 0.0014$,
GRS [44] $\alpha_s(M_Z^2) = 0.111$,
MRST03 [66] $\alpha_s(M_Z^2) = 0.1153 \pm 0.0020$,
SY01(ep) [69] $\alpha_s(M_Z^2) = 0.1166 \pm 0.0013$,
SY01(νN) [69] $\alpha_s(M_Z^2) = 0.1153 \pm 0.0063$,
A06 [49] $\alpha_s(M_Z^2) = 0.1128 \pm 0.0015$,
BBG [30] $\alpha_s(M_Z^2) = 0.1134^{+0.0019}_{-0.0021}$,
BM07 [70] $\alpha_s(M_Z^2) = 0.1189 \pm 0.0019$,
KPS00(νN) [14] $\alpha_s(M_Z^2) = 0.118 \pm 0.002(\text{stat}) \pm 0.005(\text{syst}) \pm 0.003(\text{theory})$,
KPS03(νN) [15] $\alpha_s(M_Z^2) = 0.119 \pm 0.002(\text{stat}) \pm 0.005(\text{syst}) \pm 0.002(\text{threshold})^{+0.004}_{-0.002}(\text{scale})$,

and with the value of the current world average

$$\alpha_s(M_Z^2) = 0.1189 \pm 0.0010, \tag{34}$$

which has been extracted in [71] recently.

We hope our results of QCD analysis of structure functions in terms of Jacobi polynomials could be able to describe more complicated hadron structure functions. We also hope to be able to consider the N^{3}LO corrections and massive quark contributions by using the structure function expansion in terms of the Jacobi polynomials.

ACKNOWLEDGMENTS

We are especially grateful to G. Altarelli and J. Blümlein for guidance and critical remarks. A. N. K. is grateful to S. Albino for useful discussions. We would like to thank M. Ghominejad and Z. Karamloo for reading the manuscript of this paper. A. N. K. thanks Semnan University for partial financial support of this project. We acknowledge the Institute for Studies in Theoretical Physics and Mathematics (IPM) for financially supporting this project.

[1] G. Altarelli, arXiv:0804.4147.
[2] G. Altarelli, R. D. Ball, and S. Forte, Nucl. Phys. **B799**, 199 (2008).
[3] G. Altarelli, R. D. Ball, and S. Forte, Proc. Sci., RADCOR2007 (**2007**) 028 [arXiv:0802.0968].
[4] S. Atashbar Tehrani and A. N. Khorramian, J. High Energy Phys. 07 (2007) 048.
[5] A. N. Khorramian and S. Atashbar Tehrani, J. High Energy Phys. 03 (2007) 051.
[6] G. Parisi and N. Sourlas, Nucl. Phys. **B151**, 421 (1979); I. S. Barker, C. B. Langensiepen, and G. Shaw, Nucl. Phys. **B186**, 61 (1981).
[7] I. S. Barker, B. R. Martin, and G. Shaw, Z. Phys. C **19**, 147 (1983); I. S. Barker and B. R. Martin, Z. Phys. C **24**, 255 (1984); S. P. Kurlovich, A. V. Sidorov, and N. B. Skachkov, JINR Report No. E2-89-655, Dubna, 1989.
[8] V. G. Krivokhizhin, S. P. Kurlovich, V. V. Sanadze, I. A. Savin, A. V. Sidorov, and N. B. Skachkov, Z. Phys. C **36**, 51 (1987).
[9] V. G. Krivokhizhin *et al.*, Z. Phys. C **48**, 347 (1990).
[10] J. Chyla and J. Rames, Z. Phys. C **31**, 151 (1986).
[11] I. S. Barker, C. S. Langensiepen, and G. Shaw, Nucl. Phys. **B186**, 61 (1981).
[12] A. L. Kataev, A. V. Kotikov, G. Parente, and A. V. Sidorov, Phys. Lett. B **417**, 374 (1998).
[13] A. L. Kataev, G. Parente, and A. V. Sidorov, *Proceedings of Quarks '98* edited by F. L. Bezrukov, V. A. Matveev, V. A. Rubakov, A. N. Tavkhelidze, and S. V. Troitsky (INR

Press, Moscow, Russia, 1999), pp. 90-103, arXiv:hep-ph/9809500.
[14] A. L. Kataev, G. Parente, and A. V. Sidorov, Nucl. Phys. **B573**, 405 (2000).
[15] A. L. Kataev, G. Parente, and A. V. Sidorov, Phys. Part. Nucl. **34**, 20 (2003); Fiz. Elem. Chastits At. Yadra **34** 43 (2003).**38** 827(E) (2007).A. L. Kataev, G. Parente, and A. V. Sidorov, Nucl. Phys. B, Proc. Suppl. **116**, 105 (2003).
[16] A. N. Khorramian, S. A. Tehrani, and M. Ghominejad, Acta Phys. Pol. B **38**, 3551 (2007).
[17] E. Leader, A. V. Sidorov, and D. B. Stamenov, Int. J. Mod. Phys. A **13**, 5573 (1998).
[18] A. N. Khorramian and S. A. Tehrani, arXiv:0712.2373.
[19] A. N. Khorramian and S. Atashbar Tehrani, AIP Conf. Proc. **915**, 420 (2007).
[20] A. Mirjalili, A. N. Khorramian, and S. Atashbar-Tehrani, Nucl. Phys. B, Proc. Suppl. **164**, 38 (2007).
[21] A. Mirjalili, S. Atashbar Tehrani, and A. N. Khorramian, Int. J. Mod. Phys. A **21**, 4599 (2006).
[22] W. L. van Neerven and A. Vogt, Nucl. Phys. **B568**, 263 (2000).
[23] W. L. van Neerven and A. Vogt, Nucl. Phys. **B588**, 345 (2000).
[24] J. Blümlein and A. Vogt, Phys. Rev. D **58**, 014020 (1998).
[25] M. Gluck, C. Pisano, and E. Reya, Eur. Phys. J. C **50**, 29 (2007).
[26] J. A. M. Vermaseren, A. Vogt, and S. Moch, Nucl. Phys. **B724**, 3 (2005).
[27] R. S. Towell *et al.* (E866 Collaboration), Phys. Rev. D **64**, 052002 (2001).
[28] A. D. Martin *et al.*, Eur. Phys. J. C **23**, 73 (2002).
[29] J. Blümlein, H. Böttcher, and A. Guffanti, Nucl. Phys. B, Proc. Suppl. **135**, 152 (2004).
[30] J. Blumlein, H. Bottcher, and A. Guffanti, Nucl. Phys. **B774**, 182 (2007).
[31] W. Furmanski and R. Petronzio, Z. Phys. C **11**, 293 (1982).
[32] W. L. van Neerven and E. B. Zijlstra, Phys. Lett. B **272**, 127 (1991); E. B. Zijlstra and W. L. van Neerven, Nucl. Phys. **B383**, 525 (1992).
[33] O. V. Tarasov, A. A. Vladimirov, and A. Y. Zharkov, Phys. Lett. **93B**, 429 (1980).
[34] S. A. Larin and J. A. M. Vermaseren, Phys. Lett. B **303**, 334 (1993).
[35] A. Vogt, Comput. Phys. Commun. **170**, 65 (2005).
[36] A. C. Benvenuti *et al.* (BCDMS Collaboration), Phys. Lett. B **237**, 592 (1990); A. C. Benvenuti *et al.* (BCDMS Collaboration), Phys. Lett. B **223**, 485 (1989); **237**, 592 (1990); **237**, 599 (1990).
[37] L. W. Whitlow, E. M. Riordan, S. Dasu, S. Rock, and A. Bodek, Phys. Lett. B **282**, 475 (1992).
[38] M. Arneodo *et al.* (New Muon Collaboration), Nucl. Phys. **B483**, 3 (1997).
[39] C. Adloff *et al.* (H1 Collaboration), Eur. Phys. J. C **21**, 33 (2001); **30**, 1 (2003).
[40] J. Breitweg *et al.* (ZEUS Collaboration), Eur. Phys. J. C **7**, 609 (1999); S. Chekanov *et al.* (ZEUS Collaboration), Eur. Phys. J. C **21**, 443 (2001).
[41] D. Stump *et al.*, Phys. Rev. D **65**, 014012 (2001).
[42] F. James, CERN Program Library, Long Writeup D506 (MINUIT).
[43] H. Georgi and H. D. Politzer, Phys. Rev. D **14**, 1829 (1976).
[44] M. Gluck, E. Reya, and C. Schuck, Nucl. Phys. **B754**, 178 (2006).
[45] S. Alekhin, Pis'ma Zh. Eksp. Teor. Fiz. **82**, 710 (2005) [JETP Lett. **82**, 628 (2005)].
[46] A. D. Martin, W. J. Stirling, R. S. Thorne, and G. Watt, Phys. Lett. B **652**, 292 (2007).
[47] A. D. Martin, R. G. Roberts, W. J. Stirling, and R. S. Thorne, Phys. Lett. B **604**, 61 (2004).
[48] S. Alekhin, Phys. Rev. D **68**, 014002 (2003).
[49] S. Alekhin, K. Melnikov, and F. Petriello, Phys. Rev. D **74**, 054033 (2006).
[50] U. K. Yang and A. Bodek, Eur. Phys. J. C **13**, 241 (2000).
[51] J. Blumlein and H. Bottcher, Phys. Lett. B **662**, 336 (2008).
[52] Program summary, http://particles.ipm.ir/QCD.htm.
[53] R. S. Towell *et al.* (FNAL E866/NuSea Collaboration), Phys. Rev. D **64**, 052002 (2001).
[54] P. Amaudruz *et al.* (New Muon Collaboration), Phys. Rev. Lett. **66**, 2712 (1991); M. Arneodo *et al.* (New Muon Collaboration), Phys. Rev. D **50**, R1 (1994); M. Arneodo *et al.* (New Muon Collaboration), Nucl. Phys. **B487**, 3 (1997).
[55] K. Gottfried, Phys. Rev. Lett. **18**, 1174 (1967).
[56] A. L. Kataev and G. Parente, Phys. Lett. B **566**, 120 (2003).
[57] A. L. Kataev, arXiv:hep-ph/0311091.
[58] D. J. Broadhurst, A. L. Kataev, and C. J. Maxwell, Phys. Lett. B **590**, 76 (2004).
[59] D. J. Broadhurst, A. L. Kataev, and C. J. Maxwell, arXiv:hep-ph/0410058.
[60] A. L. Kataev, Phys. Part. Nucl. **36**, S168 (2005).
[61] A. L. Kataev, Proc. Sci., ACAT2007 (2007) 072 [arXiv:0707.2855].
[62] R. Abbate and S. Forte, Phys. Rev. D **72**, 117503 (2005).
[63] K. G. Chetyrkin, B. A. Kniehl, and M. Steinhauser, Phys. Rev. Lett. **79**, 2184 (1997); S. Bethke, J. Phys. G **26**, R27 (2000); W. Bernreuther and W. Wetzel, Nucl. Phys. **B197**, 228 (1982); **B513**, 758(E) (1998).
[64] S. Chekanov *et al.* (ZEUS Collaboration), Phys. Rev. D **67**, 012007 (2003).
[65] J. Pumplin, D. R. Stump, J. Huston, H. L. Lai, P. Nadolsky, and W. K. Tung, J. High Energy Phys. 07 (2002) 012.
[66] A. D. Martin, R. G. Roberts, W. J. Stirling, and R. S. Thorne, arXiv:hep-ph/0307262.
[67] V. G. Krivokhizhin and A. V. Kotikov, Yad. Fiz. **68**, 1935 (2005) [Phys. At. Nucl. **68**, 1873 (2005)].
[68] J. Blümlein and H. Böttcher, Nucl. Phys. **B636**, 225 (2002).
[69] J. Santiago and F. J. Yndurain, Nucl. Phys. **B611**, 447 (2001).
[70] P. M. Brooks and C. J. Maxwell, Nucl. Phys. **B780**, 76 (2007).
[71] S. Bethke, Prog. Part. Nucl. Phys. **58**, 351 (2007).